Monthly Notices of the ROYAL ASTRONOMICAL SOCIETY

MNRAS **547,** 1–7 (2026) https://doi.org/10.1093/mnras/stag321
Advance Access publication 2026 February 17

Is Mira B a low mass white dwarf?

R. K. Zamanov ,[1]★ V. Irincheva,[1] B. Spassov,[1] A. Kurtenkov,[1,2] D. Marchev,[3] M. Minev,[1] M. F. Bode,[4,5] L. Dankova,[1,2] B. Borisov,[3] M. Dechev[1] and G. Yordanova[3]

[1]*Institute of Astronomy and National Astronomical Observatory, Bulgarian Academy of Sciences, 72 Tsarigradsko Shose, 1784 Sofia, Bulgaria*
[2]*Faculty of Physics, Sofia University 'St. Kliment Ohridski', 5 James Bourchier Blvd., 1164 Sofia, Bulgaria*
[3]*Department of Physics and Astronomy, Shumen University 'Episkop Konstantin Preslavski', 115 Universitetska Str., 9700 Shumen, Bulgaria*
[4]*Astrophysics Research Institute, Liverpool John Moores University, IC2, 149 Brownlow Hill, Liverpool L3 5RF, UK*
[5]*Office of the Vice Chancellor, Botswana International University of Science and Technology, Private Bag 16, 10071 Palapye, Botswana*

Accepted 2026 February 12. Received 2026 February 12; in original form 2026 January 7

ABSTRACT

We report photometric observations in Johnson B and V bands of the short term variability (flickering) of Mira (omicron Ceti). The observations were performed during seven nights in the period 2025 August–October, in the course of the last minimum of the Mira pulsations. The observed peak-to-peak amplitude of the flickering is 0.11–0.28mag in B band. For the flickering source we find luminosity in the range 0.10–0.46 $L_\odot$. Using the amplitude–flux relation, we estimate an average luminosity of the accretion disc $L_d = 0.91 \pm 0.28\,L_\odot$. Assuming that the white dwarf accretes material through Wind Roche Lobe Overflow, we find that Mira B is a low mass white dwarf with $M_{wd} = 0.24 \pm 0.04\,M_\odot$ accreting at a rate $6.8 \times 10^{-9}\,M_\odot\,yr^{-1}$. This value of the mass is in the range of the extremely low mass white dwarfs. The data are available on Zenodo: https://zenodo.org/records/18756532.

Key words: accretion, accretion discs – stars: AGB and post-AGB – binaries: symbiotic – stars: individual: omi Cet.

1 INTRODUCTION

Mira (omicron Ceti, HD 14386) is a binary system consisting of an asymptotic giant branch star of spectral type M5-9III (Mira A) and a hot companion (Mira B). 'The Wonderful Star' (omicron Ceti) was identified as a variable star in 1596 (E. G. Hogg 1933). The companion (Mira B) was discovered in 1922 by A. H. Joy and R. G. Aitken (R. G. Aitken 1923) as a blue star located at an angular distance of ≈0.6 arcsec. An bow shock and turbulent wake extend over 2° on the sky, arising from Mira's large space velocity and the interaction between its strong wind and the interstellar medium. This wind wake is a tracer of the past 30 000 yr of Mira's mass-loss (D. C. Martin et al. 2007). Another part of the wind is captured by Mira B and forms a bridge between Mira A and Mira B (M. Karovska 2006).

In the recent catalogues, Mira is classified as an accreting-only symbiotic star (S. Akras et al. 2019; J. Merc, R. Gális & M. Wolf 2019), in other words it consists of a red giant star and a white dwarf companion which accretes matter from the primary component. In the older catalogues a classification as 'symbiotic-like' or 'weakly symbiotic' can also be found (e.g. K. Belczyński et al. 2000). The accretion produces rapid light-variations on a time scale minutes-hours (M. F. Walker 1957; B. Warner 1972). The amplitude of these optical brightness fluctuations is the same as those from accreting white dwarfs in Cataclysmic Variables, and significantly larger than one would expect from an accreting main sequence star and reveals Mira B to be a white dwarf (J. L. Sokoloski & L. Bildsten 2010).

Numerical models (M. Val-Borro et al. 2017) and high resolution observations (M. Karovska 2006) show that the accreting mechanism is most likely Wind Roche Lobe Overflow (WRLOF). However, J. L. Sokoloski & L. Bildsten (2010) as well as R. K. Zamanov et al. (2025) found that the accretion rate is considerably below the expected value. To shed light on this discrepancy, we performed new observations of the flickering during the 2025 minimum. These allow us to calculate the temperature and radius of the flickering source, accretion disc luminosity, and estimate the mass of Mira B.

2 OBSERVATIONS

The observations were secured with three telescopes: **(i)** the 50/70 cm Schmidt telescope (V. G. Golev, M. K. Tsvetkov & E. A. Vitrichenko 1982; M. K. Tsvetkov et al. 1987), **(ii)** the 1.5m AZ1500 telescope (E. Semkov et al. 2025) of the Rozhen National Astronomical Observatory, Bulgaria, and **(iii)** the 40 cm telescope of the Shumen University (D. Kjurkchieva et al. 2020). The three telescopes are each equipped with CCD camera and rotating filter wheel. On the 50/70 cm Schmidt telescope we used full the CCD frame which covers a field of view 71 × 71 arcmin.

Comparison stars were BD−03 356 (B = 11.140, V = 10.645) and HD 14 411 (B = 10.779, V = 9.347). For control of the data

★ E-mail: rzamanov@nao-rozhen.org

Table 1. Photometry of Mira. In the table are given: date of observation (in format YYYY-MM-DD), UT-start and UT-end of the run (in format HH:MM), band, number of the data points, minimum, maximum, average, and median magnitudes in the corresponding band, standard deviation of the mean, amplitude, typical observational error.

Date telescope	UT	Band	N_{pts}	Min (mag)	Max (mag)	Average (mag)	Median (mag)	stdev (mag)	ampl. (mag)	merr (mag)
2025-08-28	23:17–03:01	*B*	156 × 5s	9.535	9.647	9.5942	9.5950	0.026	0.112	0.004
50/70cm		*V*	157 × 3s	8.290	8.378	8.3376	8.3380	0.018	0.088	0.003
2025-08-29	22:28–02:59	*B*	186 × 5s	9.567	9.729	9.6446	9.6395	0.044	0.162	0.003
50/70cm		*V*	189 × 3s	8.326	8.425	8.3747	8.3720	0.026	0.099	0.003
2025-09-22	23:14–02:57	*B*		9.603	9.887	9.7645	9.772	0.071	0.284	0.002
			120 × 15s							
50/70cm		*V*	118 × 5s	8.533	8.690	8.6212	8.627	0.038	0.157	0.002
2025-10-19	20:40–01:08	*B*		10.152	10.335	10.2367	10.2240	0.047	0.183	0.008
			233 × 10s							
40cm		*V*	232 × 4s	8.668	8.750	8.7102	8.7065	0.020	0.082	0.009
2025-10-23	21:14–00:02	*B*	78 × 10s	10.075	10.206	10.1611	10.1710	0.035	0.131	0.008
40cm		*V*	78 × 4s	8.479	8.547	8.5173	8.5185	0.016	0.068	0.008
2025-10-29	19:14–20:45	*B*	67 × 5s	9.623	9.814	9.7066	9.6910	0.052	0.191	0.002
1.5m		*V*	67 × 1s	8.433	8.527	8.4699	8.4670	0.021	0.094	0.002
2025-10-31	22:00–23:32	*B*	110 × 5s	9.972	10.060	10.0075	10.0015	0.023	0.088	0.003
1.5m		*V*		8.536	8.609	8.5707	8.5720	0.015	0.073	0.003
			110 × 0.5s							

processing we also used HD 14 627 (B = 9.456, V = 9.004), HD 14 223 (B = 10.055, V = 9.491), and BD−03 364 (B = 10.538, V = 9.931). The magnitudes are taken from Gaia Collaboration (2022) and from U. Munari et al. (2014). The resulting light curves span from 3.7 to 4.9 h. Table 1 gives full details of each run including light-curve statistics.

In the optical *V* band Mira pulsates between $2.5 < m_V < 9.0$ magnitude (D. Hoffleit 1997; M. Gromadzki et al. 2009). As the flickering variability is related to the companion, it is essential to observe at a time when Mira A is faint, and our new data are when $m_V \geq 8.3$.

Part of our observations of omicron Ceti are plotted in Fig. 1. The intra-night variability (flickering) is evident on all nights. The peak-to-peak amplitude in *V* band is 0.09–0.16 mag, and in *B* band it is 0.11–0.28 mag. The variability in the two bands is synchronized, however the amplitude is larger in *B* band, similar to the symbiotic recurrent novae T CrB and RS Oph.

3 RESULTS

In Fig. 2(a) we plot the *B* versus *V* magnitude. Fig. 2(b) represents the colour–magnitude diagram – *B* magnitude versus $B-V$ colour. For each night the star becomes redder when it gets fainter. The positions of data on this figure are related to the brightness variations during the Mira cycle, as well as the variable luminosity of accretion disc (see Section 3.2).

The distance to Mira is estimated to be 92 ± 10 pc from the *Hipparcos* parallax (10.91 ± 1.22 arcsec) (F. Leeuwen 2007). Other values using different relations include: 105 ± 7 pc (M. W. Feast et al. 1989), 107 ± 12 pc (G. R. Knapp et al. 2003), 115 ± 7 pc (P. A. Whitelock, M. W. Feast & F. Van Leeuwen 2008). We adopt a distance of 100 pc. The interstellar extinction at this distance is less than 0.01 mag (R. Lallement et al. 2019). In such wide binary systems, the white dwarf is located outside of the dust cocoon associated with the Mira star (M. Gromadzki et al. 2009) and we hence assume no extinction for Mira B.

3.1 Flickering

For analysis of the flickering, A. Bruch (1992) suggests the light curve of the intra-night variability to be separated into two parts – constant light and variable (flickering) source. Following this procedure, we calculate the flux of the flickering light source as $F_{\rm fl1} = F_{\rm av} - F_{\rm min}$, where $F_{\rm av}$ is the average flux during the run and $F_{\rm min}$ is the minimum flux during the run (corrected for the typical error of the observations). A slightly different method is proposed by T. Nelson et al. (2011). They used for the flickering source $F_{\rm fl2} = F_{\rm max} - F_{\rm min}$, where $F_{\rm max}$ is the maximum flux during the run. In fact, the method of A. Bruch (1992) evaluates the average brightness of the flickering source, while that of T. Nelson et al. (2011) its maximal brightness. More details can be found in section 4 of A. Bruch (1992) and section 6.5 of T. Nelson et al. (2011). $F_{\rm fl1}$ and $F_{\rm fl2}$ have been calculated for each band, using the values given in Table 1. To convert the observed magnitudes in fluxes, we use the calibration for a zero magnitude star $F_0(B) = 6.13268 \times 10^{-9}$ erg cm^{-2} s^{-1} Å^{-1}, $\lambda_{\rm eff}(B) = 4371.07$ Å, $F_0(V) = 3.62708 \times 10^{-9}$ erg cm^{-2} s^{-1} Å^{-1} and $\lambda_{\rm eff}(V) = 5477.70$ Å as given in the Spanish virtual observatory Filter Profile Service (C. Rodrigo & E. Solano 2020). To calculate the temperature, we use the calibration for the $(B-V)$ colour of a blackbody (table 18 in V. Straižys 1992). Using the temperature, distance $d = 100$ pc, $F_{\rm fl1}$, and $F_{\rm fl1}$, we calculate the radius and the luminosity of the flickering source.

In Table 2 are given: the colours $(B-V)_{01}$ and $(B-V)_{02}$ of the flickering source, $T_{\rm fl1}$ and $T_{\rm fl2}$ (temperature of the flickering source), $R_{\rm fl1}$ and $R_{\rm fl2}$ (radius the flickering source), $L_{\rm fl1}$ and $L_{\rm fl2}$ (luminosity the flickering source). $(B-V)_{01}$, $T_{\rm fl1}$, $R_{,\rm fl1}$ and $L_{\rm fl1}$ are calculated using the average flux, following A. Bruch (1992), $(B-V)_{02}$, $T_{\rm fl2}$, $R_{\rm fl2}$, and $L_{\rm fl2}$ – using the maximum flux, following T. Nelson et al. (2011).

Using the method of A. Bruch (1992), we find for our runs: $(B-V)_{01}$ in the range from 0.55 to 1.1, corresponding to temperature in the range 4200–6200 K, radius of the flickering source 0.30–0.85 $R_\odot$, and luminosity 0.1–0.2 $L_\odot$. Using the method of T. Nelson et al. (2011), we find similar results for the colour and temperature: $(B-V)_{02}$ in the range from 0.5 to 1.2, corresponding to

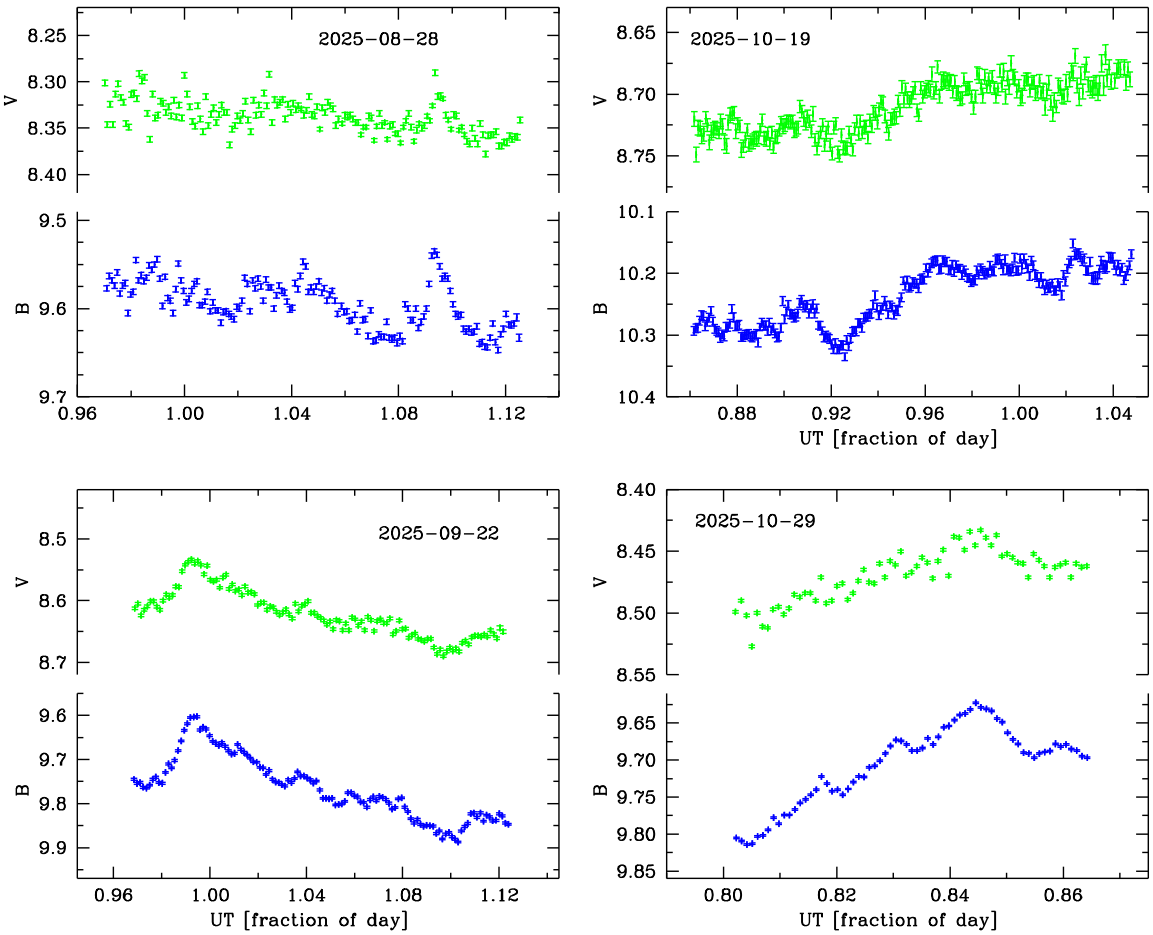

Figure 1. Short term variability of Mira in B and V bands. An intra-night variability with an amplitude $\Delta B \sim 0.15$ mag is visible. The date of observations is marked on each panel.

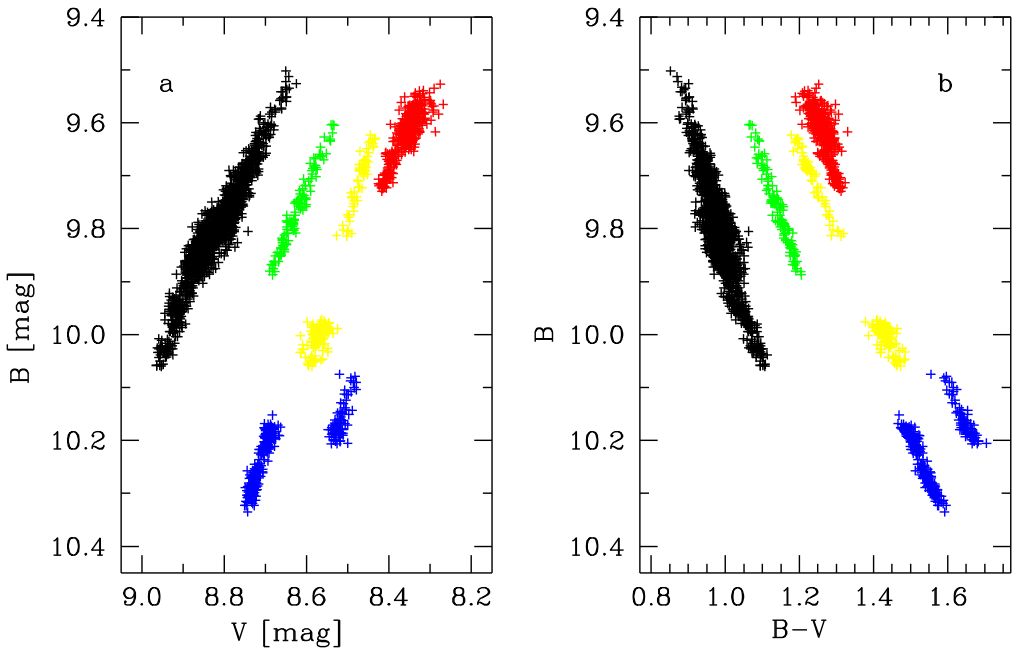

Figure 2. **(a)** B band versus V-band magnitude. **(b)** Colour magnitude diagram. The colours are as follows: data from 2024–11 (black), 2025-08-28 and 2025-08-29 (red), 2025-09-22 (green), 2025-10-19 and 2025-10-23 (blue), 2025-10-29 and 2025-10-31 (yellow).

Table 2. Flickering source of Mira B. $(B-V)_{01}$, T_1, R_{fl1}, and L_{fl1} are dereddened colour, temperature, radius, and luminosity of the flickering source calculated following Bruch (1992), $(B-V)_{02}$, T_2, R_{fl2}, and L_{fl2} – following Nelson et al. (2011), see Section 3 for details.

Date	$(B-V)_{01}$	T_1 (K)	R_{fl1} [$R_\odot$]	L_{fl1} ($L_\odot$)	$(B-V)_{02}$	T_2 (K)	R_{fl2} ($R_\odot$)	L_{fl2} ($L_\odot$)
2025-08-28	0.9721	4439	0.7671	0.205	0.9950	4375	1.1960	0.470
2025-08-29	0.7248	5342	0.5024	0.184	0.7372	5285	0.7328	0.376
2025-09-22	0.5434	6229	0.3656	0.180	0.4878	6576	0.5028	0.424
2025-10-19	0.5738	6039	0.2880	0.099	0.6619	5628	0.4895	0.216
2025-10-23	0.9606	4471	0.5315	0.101	0.818	4941	0.6525	0.228
2025-10-29	0.5756	6028	0.3854	0.176	0.468	6702	0.3978	0.286
2025-10-31	1.1014	4079	0.8773	0.191	1.220	3770	1.5944	0.460

Table 3. Accretion disc luminosity, L_d of Mira B. The first column gives date of observation. The second and the third columns give the estimated L_d using equations (1) and (2), respectively (see Section 3 for details).

Date	L_d ($L_\odot$) from equation (1)	L_d ($L_\odot$) from equation (2)
2018-09-07	0.345	0.584
2018-09-09	0.439	0.977
2024-11-24	1.163	1.165
2024-11-25	0.787	0.861
2024-11-26	1.012	0.992
2024-11-27	0.983	1.358
2025-08-28	1.132	1.298
2025-08-29	1.018	1.038
2025-09-22	0.997	1.172
2025-10-19	0.547	0.595
2025-10-23	0.559	0.629
2025-10-29	0.972	0.791
2025-10-31	1.056	1.272
Average	0.91 ± 0.28	

temperature in the range 3800–6600 K. The method of T. Nelson et al. (2011) gives larger values for the radius (0.4–1.5 $R_\odot$) and for the luminosity (0.22–0.46 $L_\odot$), because it refers to the maximal brightness.

3.2 Optical luminosity of Mira B

The variability generated in accretion discs produces light curves that are phenomenologically similar across active galactic nuclei, X-ray binaries, and accreting white dwarfs. There is an amplitude–flux relation, which is a result of the universality of the accretion physics from proto-stars still in the star-forming process to the supermassive black holes at the centres of galaxies (e.g. P. Uttley, I. M. McHardy & S. Vaughan 2005; S. Scaringi et al. 2015; C. Koen 2016, and references therein). This relation is probably connected with the viscosity (A. R. King et al. 2004). To estimate the luminosity of the accretion disc around the white dwarf, we use the observed relationship between the amplitude of the flickering (ΔF) and the average flux F_{av}. For accreting white dwarfs these two parameters are connected as $\Delta F/F_{av} = 0.362 \pm 0.045$ (R. K. Zamanov et al. 2016). From this amplitude-flux relation, we adopt

$$2L_{fl1} = 0.362\, L_d, \quad (1)$$
$$L_{fl2} = 0.362\, L_d, \quad (2)$$

where L_d is the accretion disc luminosity. In Table 3 is given the calculated L_d for the past flickering observations (R. Zamanov et al. 2019; R. K. Zamanov et al. 2025), as well as the new data. The calculated luminosity of the accretion disc is in the range from 0.4 to 1.3 $L_\odot$, with average $L_d = 0.91 \pm 0.28\ L_\odot$.

3.3 Accretion luminosity of Mira B

The luminosity of the accretion disc of an accreting white dwarf depends on the mass of the white dwarf, its radius, and the mass accretion rate:

$$L_d = \frac{G\, M_{wd}\, \dot{M}_a}{2\, R_{wd}}, \quad (3)$$

where $\dot{M}_a$ is the mass accretion rate, M_{wd} is the mass of the white dwarf, R_{wd} is the radius of the white dwarf. For a standard accretion disc, the disc luminosity is half of the total accretion luminosity. The other half is emitted by the boundary layer between the accretion disc and the white dwarf.

A characteristic feature of the white dwarfs is that the less massive white dwarfs have larger radii. For the radius of the white dwarf, we use the formula by P. Eggleton as given in F. Verbunt & S. Rappaport (1988):

$$\frac{R_{wd}}{R_\odot} = 0.0114 \left[\left(\frac{M_{wd}}{M_{Ch}}\right)^{-2/3} - \left(\frac{M_{wd}}{M_{Ch}}\right)^{2/3} \right]^{1/2} \times \left[1 + 3.5 \left(\frac{M_{wd}}{M_p}\right)^{-2/3} + \left(\frac{M_{wd}}{M_p}\right)^{-1} \right]^{-2/3}, \quad (4)$$

where M_p is a constant $M_p = 0.00057\, M_\odot$, $M_{Ch} = 1.44\, M_\odot$ is the Chandrasekhar mass limit for a white dwarf. We note in passing that the observed masses and radii of white dwarfs agree with this formula (e.g. K. Bartnick et al. 2025, and references therein). This mass–radius relation gives radius $R_{wd} = 8614$ km for a $M_{wd} = 0.6\, M_\odot$, $R_{wd} = 10675$ km for a $M_{wd} = 0.4\, M_\odot$, $R_{wd} = 14075$ km for a $M_{wd} = 0.2\, M_\odot$.

3.4 Bondi–Hoyle–Lyttleton accretion

The orbital period of Mira A+B binary is $\geq$500 yr. In such wide binaries the white dwarf captures a fraction of the wind of the red giant. In standard Bondi–Hoyle–Lyttleton wind accretion (for a review, see R. Edgar 2004), the accretion rate on to the white dwarf depends on the orbital and stellar parameters (F. Hoyle & R. A. Lyttleton 1939; H. Bondi & F. Hoyle 1944):

$$\dot{M}_{acc} = \frac{R_a^2}{4\, a^2}\, \dot{M}_w\ , \quad (5)$$

where $\dot{M}_w$ is the wind mass-loss rate of the red giant (Mira A), a is the semimajor axis of the binary orbit, R_a is the accretion radius of the white dwarf:

$$R_a = \frac{2\,G\,M_{wd}}{v_w^2 + v_{orb}^2 + c_s^2}\,, \tag{6}$$

where v_w is the wind velocity, v_{orb} is the orbital velocity, c_s is the speed of sound in the wind at distance a. We adopt $c_s = 1\,km\,s^{-1}$ (C. Sandin & L. Mattsson 2020). The semimajor axis is related to the orbital period by the Kepler's third law:

$$P_{orb}^2 = \frac{4\,\pi^2\,a^3}{G\,(M_1 + M_{wd})}\,, \tag{7}$$

where M_1 is the mass of the red giant primary (Mira A). The orbital velocity of the white dwarf v_{orb} is

$$v_{orb} = \frac{2\,\pi\,M_1\,a}{(M_1 + M_{wd})\,P_{orb}}. \tag{8}$$

For the mass-loss rate of Mira A, we adopt $M_w = 4.4 \times 10^{-7}\,M_\odot\,yr^{-1}$ and $v_w = 6.7\,km\,s^{-1}$ (G. R. Knapp et al. 1998). Omicron Ceti is a very wide binary system. S. Snaid et al. (2018) collected data for Mira B positions relative to Mira A and fitted them with a circular orbit inclined at $i = 67^0$, with period 945 yr and angular separation 1.03 arcsec. For a distance $d = 100$ pc, it gives a physical separation between Mira A and B of $a = 103$ au.

Using equation (7) and the observed parameters P_{orb} and a we estimate the mass of the system. We calculate the orbital velocity V_{orb} via equation (8) for a range of white dwarf masses (from 0.1 to 1.43 $M_\odot$). We use equations (5) and (6) to estimate the mass acretion rate $\dot{M}_{acc}$. The radius of the white dwarf for each mass is calculated via equation (4) and then the accretion luminosity L_d is obtained from equation (3). We compare the resulting values for L_d with the value derived from our observations and achieve agreement at $M_{wd} = 0.42 \pm 0.02\,M_\odot$ and $M_1 \approx 0.8\,M_\odot$. Such a white dwarf will accrete at a rate $\dot{M}_a \approx 2.1 \times 10^{-9}\,M_\odot\,yr^{-1}$ and will emit $L_d \approx 0.93\,L_\odot$.

3.5 Wind Roche Lobe Overflow (WRLOF)

Wind Lobe Overflow (WRLOF) is proposed by S. Mohamed & P. Podsiadlowski (2007) for symbiotic binaries. This is a mass-transfer mechanism where the stellar wind (particularly if it is dense and slow), fills the Roche lobe of the red giant and is transferred to the hot component through the inner Lagrangian point. This mechanism is a hybrid between the normal Roche lobe overflow and standard wind accretion (Bondi–Hoyle–Lyttleton accretion). Numerical simulations (S. Mohamed & P. Podsiadlowski 2012; M. Val-Borro et al. 2017) have shown that in case of WRLOF the subsequent mass-transfer rate is at least an order of magnitude greater than the analogous Bondi–Hoyle–Lyttleton value. Here we will assume that it is 10–20 times greater.

In agreement with WRLOF scenario, the high resolution *Chandra* and *Hubble Space telescope* observations have shown that in the mass exchange between Mira A and Mira B in addition to wind accretion there is evidence for Roche lobe like overflow (M. Karovska et al. 2005; M. Karovska 2006).

Assuming that in case of WRLOF the mass accretion rate is 10 times higher than the standard Bondi–Hoyle–Lyttleton value, and using the above equations we find that a white dwarf having accretion disc luminosity $L_d \approx 0.91\,L_\odot$ accreting through WRLOF, has to be a low mass, with $M_{wd} = 0.21 \pm 0.02$. This value of the mass is the lower limit because in equation (3) the inclination of the accretion disc is not taken into account. If we adopt $L_d = 0.5\,G\,M_{wd}\,\dot{M}_a\,\cos i\,R_{wd}^{-1}$ and $i = 67^0$, then we get $M_{wd} = 0.28\,M_\odot$ for a WRLOF with 10 times higher accretion rate than Bondi–Hoyle–Lyttleton accretion and $M_{wd} = 0.23\,M_\odot$ for a WRLOF with a 20 times higher accretion rate.

The WRLOF mechanism suggests that Mira B is a low mass white dwarf with mass $0.24 \pm 0.04\,M_\odot$ accreting at a rate of $6.8 \times 10^{-9}\,M_\odot\,yr^{-1}$. In other words the white dwarf captures ≈1.5 per cent of the wind of the giant.

4 DISCUSSION

Here, we explore how varying various critical parameters affects our overall conclusions. Symbiotic Miras in general have very long orbital periods, longer than 100 yr (K. H. Hinkle et al. 2013). In Section 3, we used $P_{orb} = 945$ yr (S. Snaid et al. 2018). Earlier estimates give shorter periods: 498 yr (J. L. Prieur et al. 2002) and 610 yr (M. J. Ireland et al. 2007). If we assume $P_{orb} = 610$ yr, than we get an almost identical value of $M_{wd} = 0.24\,M_\odot$, because this will change v_{orb}. However the main factor in equation (6) is v_w.

In Section 3, we used speed of sound $c_s = 1.0\,km\,s^{-1}$. If we assume a two times larger value $c_s = 2.0\ km\,s^{-1}$ or two times smaller value $c_s = 0.5\,km\,s^{-1}$ the result will be practically the same because the motion of the accreting object is supersonic and the c_s is a minor factor in equation (6).

If we use two times lower mass-loss rate of Mira A, $M_w = 2.2 \times 10^{-7}\,M_\odot\,yr^{-1}$, and $v_w = 6.7\,km\,s^{-1}$, we get the mass of the white dwarf ≈0.27 $M_\odot$. If we use different values for the mass-loss of Mira A, $M_w = 3.6 \times 10^{-7}\,M_\odot\,yr^{-1}$ and $v_w = 4.8\,km\,s^{-1}$ as given by A. M. Heras & S. Hony (2005), we derive an even lower mass of the white dwarf ≈0.17 $M_\odot$.

Significant changes in the accretion rate have been inferred in the past for Mira B (B. E. Wood & M. Karovska 2006). We also detect variations in the disc luminosity in the range $0.3 \le L_d \le 1.4\,L_\odot$ (see Table 3). The amplitude of the flickering in B band in our observations is 0.1–0.28 mag, which is similar to the amplitudes 0.15–0.30 mag observed by J. L. Sokoloski & L. Bildsten (2010).

In wide binaries as Mira A+B, the white dwarf accretes material via gravitational capture of the red-giant wind. J. L. Sokoloski & L. Bildsten (2010) estimated $\dot{M}_a \sim 10^{-10}\,M_\odot\,yr^{-1}$ assuming $M_{wd} = 0.6\,M_\odot$. S. Snaid et al. (2018) also assume $M_{wd} = 0.6\,M_\odot$. This assumption was first made by D. Reimers & A. Cassatella (1985) on the basis that two thirds of the DA white dwarfs have masses in a narrow range $0.58 \pm 0.10\,M_\odot$ (D. Koester, H. Schulz & V. Weidemann 1979). Our estimate indicates that in fact the white dwarf companion (Mira B) is a lower mass white dwarf $M_{wd} \approx 0.42\,M_\odot$ (in the case of Bondi–Hoyle–Lyttleton accretion) and a more likely value $M_{wd} \approx 0.24\,M_\odot$ (in the case of WRLOF). The result explains some early findings that the mass accretion rate is below the theretical value for WRLOF and even for Bondi–Hoyle–Lyttleton accretion (see section 5 in J. L. Sokoloski & L. Bildsten 2010). We consider the value obtained suggesting WRLOF is more probable, because the high resolution observations have shown that in the mass exchange between Mira A and Mira B there is evidence for Roche lobe like overflow (M. Karovska et al. 2005; M. Karovska 2006). We note that M. Jura & D. J. Helfand (1984) suggested that the low X-ray emission of the system can be explained if the secondary component is either a main-sequence red dwarf or an extremely low mass white dwarf. Our result is in agreement with the suggestion for a low mass white dwarf.

Having in mind our favoured result $M_{\rm wd} = 0.24\,{\rm M}_{\odot}$ and using equation (7), we estimate mass of Mira A, $M_1 \approx 1\,{\rm M}_{\odot}$. This value is highly sensitive to the adopted orbital period. If we assume $P_{\rm orb} = 610$ yr, we find $M_1 \approx 2.7\,{\rm M}_{\odot}$. Nevertheless, both values are in the range of masses of the stars on the asymptotic giant branch 0.5–4 $\rm M_{\odot}$ (E. Vassiliadis & P. R. Wood 1993).

J. Liebert, P. Bergeron & J. B. Holberg (2005) studied a sample of 348 white dwarfs from the Palomar Green Survey and obtained a mass distribution showing a main peak centred near 0.6 $\rm M_{\odot}$, a low-mass component centred near 0.4 $\rm M_{\odot}$, and a high-mass component above about 0.8 $\rm M_{\odot}$. Our result for the mass of Mira B ($M_{\rm wd} \approx 0.42\,{\rm M}_{\odot}$, assuming Bondi–Hoyle–Lyttleton accretion) is close to the low-mass component peak of the Palomar Green Survey distribution. If we assume WRLOF accretion, we obtain a value of 0.24 $\rm M_{\odot}$ for the mass of the white dwarf, which is below the lowest mass (0.32 $\rm M_{\odot}$) observed in the Palomar Green white dwarfs. More resent surveys, have shown that white dwarfs with mass less than 0.3 $\rm M_{\odot}$ do exist. In the Gaia DR2 there are 5762 extremely low mass white dwarf candidates with masses below 0.3 $\rm M_{\odot}$ (I. Pelisoli & J. Vos 2019). M. Kilic et al. (2007) reported that there are four white dwarfs from the SDSS with masses even below 0.2 $\rm M_{\odot}$.

The numerical simulations, high resolution observations as well as our results indicate that Mira B is most likely part of the group of extremely low mass white dwarfs.

5 CONCLUSIONS

We report 22.3 hours of simultaneous observations in *B* and *V* bands of the flickering of Mira obtained with the telescopes of National Astronomical Observatory Rozhen and Shumen University, Bulgaria. The observations were performed during 2025 August–October. The amplitude of the flickering was 0.11–0.28 mag in *B* band. We find that the average luminosity of the accretion disc around Mira B is $0.91 \pm 0.28\,{\rm L}_{\odot}$. Combining the equations for disc luminosity, mass accretion rate, and mass–radius relation for white dwarfs, we estimate that the white dwarf companion (Mira B) is a low mass white dwarf with $M_{\rm wd} \approx 0.42 \pm 0.04\,{\rm M}_{\odot}$ in the case of Bondi–Hoyle–Lyttleton accretion or an extremely low mass white dwarf with $M_{\rm wd} \approx 0.24 \pm 0.04\,{\rm M}_{\odot}$ in the case of WRLOF.

ACKNOWLEDGEMENTS

This work is part of the project KP-06-H98/8 'Accretion flows in binary stars' (Bulgarian National Science fund). The research infrastructure is supported by the National Roadmap for Research Infrastructure coordinated by the Ministry of Education and Science of Bulgaria. DM, BB, and GY acknowledge Scientific Research Fund of Shumen University. We thank an anonymous referee for making very valuable suggestions.

DATA AVAILABILITY

The data are available for download at zenodo.org/records/18756532.

REFERENCES

Aitken R. G., 1923, PASP, 35, 323
Akras S., Guzman-Ramirez L., Leal-Ferreira M. L., Ramos-Larios G., 2019, ApJS, 240, 21
Bartnick K., Koester D., Kudritzki R.-P., Springmann K., Stelzl S., Weiler A., 2025, MNRAS, 545, staf1811
Belczyński K., Mikołajewska J., Munari U., Ivison R. J., Friedjung M., 2000, A&AS, 146, 407
Bondi H., Hoyle F., 1944, MNRAS, 104, 273
Bruch A., 1992, A&A, 266, 237
Edgar R., 2004, New Astron. Rev., 48, 843
Feast M. W., Glass I. S., Whitelock P. A., Catchpole R. M., 1989, MNRAS, 241, 375
GAIA Collaboration et al., 2022, A&A, 674, A1
Golev V. G., Tsvetkov M. K., Vitrichenko E. A., 1982, Bolgarska Akademiia Nauk Doklady, 35, 729
Gromadzki M., Mikołajewska J., Whitelock P., Marang F., 2009, Acta Astron., 59, 169
Heras A. M., Hony S., 2005, A&A, 439, 171
Hinkle K. H., Fekel F. C., Joyce R. R., Wood P., 2013, ApJ, 770, 28
Hoffleit D., 1997, J. AAVSO, 25, 115
Hogg E. G., 1933, J. R. Astron. Soc. Can., 27, 75
Hoyle F., Lyttleton R. A., 1939, Proc. Camb. Phil. Soc. 35, 405
Ireland M. J. et al., 2007, ApJ, 662, 651
Jura M., Helfand D. J., 1984, ApJ, 287, 785
Karovska M., 2006, in Wilson A., ed., ESA SP-604: The X-ray Universe 2005. ESA, Noordwijk, p. 183
Karovska M., Schlegel E., Hack W., Raymond J. C., Wood B. E., 2005, ApJ, 623, L137
Kilic M., Allende Prieto C., Brown W. R., Koester D., 2007, ApJ, 660, 1451
King A. R., Pringle J. E., West R. G., Livio M., 2004, MNRAS, 348, 111
Kjurkchieva D., Marchev D., Borisov B., Ibryamov S., Dimitrov D., Popov V., Milev A., Petrov N., 2020, Bulg. Astron. J., 32, 113
Knapp G. R., Young K., Lee E., Jorissen A., 1998, ApJS, 117, 209
Knapp G. R., Pourbaix D., Platais I., Jorissen A., 2003, A&A, 403, 993
Koen C., 2016, A&A, 593, L17
Koester D., Schulz H., Weidemann V., 1979, A&A, 76, 262
Lallement R., Babusiaux C., Vergely J. L., Katz D., Arenou F., Valette B., Hottier C., Capitanio L., 2019, A&A, 625, A135
van Leeuwen F., 2007, A&A, 474, 653
Liebert J., Bergeron P., Holberg J. B., 2005, ApJS, 156, 47
Martin D. C. et al., 2007, Nature, 448, 780
Merc J., Gális R., Wolf M., 2019, Astron. Nachr., 340, 598
Mohamed S., Podsiadlowski P., 2007, in Napiwotzki R., Burleigh M. R., eds, ASP Conf. Ser. Vol. 372, 15th European Workshop on White Dwarfs. Astron. Soc. Pac., San Francisco, p. 397
Mohamed S., Podsiadlowski P., 2012, Balt. Astron., 21, 88
Munari U. et al., 2014, AJ, 148, 81
Nelson T., Mukai K., Orio M., Luna G. J. M., Sokoloski J. L., 2011, ApJ, 737, 7
Pelisoli I., Vos J., 2019, MNRAS, 488, 2892
Prieur J. L., Aristidi E., Lopez B., Scardia M., Mignard F., Carbillet M., 2002, ApJS, 139, 249
Reimers D., Cassatella A., 1985, ApJ, 297, 275
Rodrigo C., Solano E., 2020, XIV.0 Scientific Meeting (virtual) of the Spanish Astronomical Society. Sociedad Española de Astronomía SEA, Spain, p. 182
Sandin C., Mattsson L., 2020, MNRAS, 499, 1531
Scaringi S. et al., 2015, Sci. Adv, 1, e1500686
Semkov E. et al., 2025, C. R. Acad. Bulg. Sci., 78, 797
Snaid S., Zijlstra A. A., McDonald I., Barker H., Marsh T. R., Dhillon V. S., 2018, MNRAS, 477, 4200
Sokoloski J. L., Bildsten L., 2010, ApJ, 723, 1188
Straižys V., 1992, Multicolor Stellar Photometry. Pachart Pub House, Tucson, USA
Tsvetkov M. K., Georgiev T. B., Bilkina B. P., Tsvetkova A. G., Semkov E. H., 1987, Bolgarska Akademiia Nauk Doklady, 40, 9
Uttley P., McHardy I. M., Vaughan S., 2005, MNRAS, 359, 345

de Val-Borro M., Karovska M., Sasselov D. D., Stone J. M., 2017, MNRAS, 468, 3408
Vassiliadis E., Wood P. R., 1993, ApJ, 413, 641
Verbunt F., Rappaport S., 1988, ApJ, 332, 193
Walker M. F., 1957, in Herbig G. H., ed., IAU Symposium Vo. 3, Non-stable Stars. Cambridge Univ. Press, Cambridge, p. 46
Warner B., 1972, MNRAS, 159, 95
Whitelock P. A., Feast M. W., Van Leeuwen F., 2008, MNRAS, 386, 313
Wood B. E., Karovska M., 2006, ApJ, 649, 410
Zamanov R., Boeva S., Spassov B., Latev G., Wolter U., Stoyanov K. A., 2019, Bulg. Astron. J, 31, 110
Zamanov R. K. et al., 2016, MNRAS, 457, L10
Zamanov R. K., Spassov B., Konstantinova-Antova R., Moyseev M., Marti J., Bode M. F., Vujcic V., Sreckovic V., 2025, New Astron., 121, 102452

This paper has been typeset from a TEX/LATEX file prepared by the author.